RESEARCH ARTICLE

A connectome-based approach to assess motor outcome after neonatal arterial ischemic stroke

Mariam Al Harrach[1,2] (iD), Pablo Pretzel[3], Samuel Groeschel[3], François Rousseau[4],
Thijs Dhollander[5] (iD), Lucie Hertz-Pannier[6], Julien Lefevre[7], Stéphane Chabrier[8,9],
Mickael Dinomais[1,10] & the AVCnn study group[,a]

[1]Université d'Angers, Laboratoire Angevin de Recherche en Ingénierie des Systèmes (LARIS) EA7315, Angers, 49000, France
[2]Université de Rennes 1, Laboratoire Traitement du Signal et de l'Image (LTSI), INSERM U1099, Rennes, F-35000, France
[3]Experimental Paediatric Neuroimaging, Department of Child Neurology, University Hospital Tübingen, Tübingen, Germany
[4]IMT Atlantique, INSERM U1101 LaTIM, UBL, Brest, 29200, France
[5]Developmental Imaging, Murdoch Children's Research Institute, Melbourne, Australia
[6]UNIACT, Neurospin, Institut Joliot, CEA-Paris Saclay, Inserm U114, Université de Paris, Gif sur Yvette, F-91191, France
[7]Institut de Neurosciences de la Timone, UMR 7289, Aix Marseille Université, CNRS, Marseille, 13385, France
[8]INSERM, UMR1059 Sainbiose, Univ Saint-Étienne, Univ Lyon, Saint-Étienne, F-42023, France
[9]Paediatric Physical and Rehabilitation Medicine Department, CHU Saint-Étienne, French Centre for Paediatric Stroke, INSERM, CIC 1408, Saint-Étienne, F-42055, France
[10]Département de Médecine Physique et de Réadaptions and LUNAM, CHU Angers, Angers, France

Correspondence
Mariam Al Harrach, Laboratoire de Traitement du Signal et de l'Image (LTSI), Université de Rennes 1, Campus de Beaulieu, bat 22, F-35000 Rennes, France. Tel: +33 2 23 23 56 05; Fax: (33) 2 23 23 69 17; E-mail : mariam.al-harrach@inserm.fr

Abstract

Objective: Studies of motor outcome after Neonatal Arterial Ischemic Stroke (NAIS) often rely on lesion mapping using MRI. However, clinical measurements indicate that motor deficit can be different than what would solely be anticipated by the lesion extent and location. Because this may be explained by the cortical disconnections between motor areas due to necrosis following the stroke, the investigation of the motor network can help in the understanding of visual inspection and outcome discrepancy. In this study, we propose to examine the structural connectivity between motor areas in NAIS patients compared to healthy controls in order to define the cortical and subcortical connections that can reflect the motor outcome. **Methods:** Thirty healthy controls and 32 NAIS patients with and without Cerebral Palsy (CP) underwent MRI acquisition and manual assessment. The connectome of all participants was obtained from T1-weighted and diffusion-weighted imaging. **Results:** Significant disconnections in the lesioned and contra-lesioned hemispheres of patients were found. Furthermore, significant correlations were detected between the structural connectivity metric of specific motor areas and manuality assessed by the Box and Block Test (BBT) scores in patients. **Interpretation:** Using the connectivity measures of these links, the BBT score can be estimated using a multiple linear regression model. In addition, the presence or not of CP can also be predicted using the KNN classification algorithm. According to our results, the structural connectome can be an asset in the estimation of gross manual dexterity and can help uncover structural changes between brain regions related to NAIS.

Introduction

Neonatal Arterial Ischemic Stroke (NAIS), affecting 1 in 3200 births, is defined as a cerebro-vascular accident taking place between birth and 28 days of life with clinical or radiological evidence of focal arterial infarction.[1–3] It is recognized as a major cause of early brain injury and lasting disability[1,3] and is found to be the prominent cause of unilateral cerebral palsy (CP) in term-born children.[4] Moreover, studies demonstrated that at least two-thirds of patients will exhibit some neurodevelopmental disabilities at school-age.[5,6]

Many studies attempted to identify the predictors of motor impairment in stroke using various neurological and imaging methods that ranged from lesion localization and characterization (voxel-wise lesion symptom mapping (VLSM)) to motor system analysis using functional and structural data collected from MRI, fMRI, and diffusion tensor imaging (DTI) techniques[6–10] Recent studies proposed new biomarkers for motor outcome following stroke. These biomarkers included corticospinal tract (CST) lesion measures such as the study of Feng et al.[11] that proposed a weighted CST lesion load depicting the weight of the lesion on the CST tract. However, this study only focused on the outcome at 3 months poststroke. Another work proposed by Yoo et al. attempted to predict patients' hand function following stroke by inspecting the fiber number and fractional anisotropy in different parts of the CST.[12] However, their study was limited due to the lack of quantitative tools for the assessment of hand function. Some studies attempted to analyze the stroke motor outcome by inspecting both structural and functional measures of the motor systems.[13] They found that each of these biomarkers provide distinct information about the outcome. Nevertheless, Lin et al. demonstrated that functional connectivity measures were weaker than CST-based ones in the prediction of motor recovery.[14] Very recent studies demonstrated that the stroke volume measured shortly after the manifestation of stroke and the Alberta Stroke Program Early Computed Tomography Score (ASPECTS) in newborns were found to predict cerebral palsy as well as other neurological impairments.[15,16]

During the last decade, connectivity-based studies have emerged in the context of stroke in general.[17,18] These studies included functional, effective, and structural connectivity analysis in order to investigate the stroke's impact on brain connections and understand the process recovery after stroke.[17–21] They demonstrated that connectivity-based approaches unveils information about the reorganization of brain network poststroke which can improve prognosis as well as therapeutic interventions for rehabilitation.[20,21] In the particular case of perinatal stroke, various studies investigated the impact of the stroke on the functional connectivity in the motor,[22] sensory-motor,[23] and language network[24] as well as on the executive functions.[25] All these studies conclude on the importance of connectivity and connection reorganization in the treatment plan.

Overall structural connectomics studies have proven to be valuable in understanding brain structure,[26] disorders,[27] and development.[28] In particular, cortical disconnections of specific areas were found to be related to clinical deficits.[29,30] These studies demonstrated that connectome-based analysis can establish a relation between cortical areas connections and a clinical outcome (score).[29,30] Despite this, there is still a lack of structural connectivity-based studies of motor functions in childhood stroke and even more in NAIS.

For this purpose, we aimed to investigate the structural connectivity of the motor system's cortical and subcortical regions following NAIS in comparison to healthy controls in order to determine the cortical connections that describe the motor outcome at 7 years. The motor outcome was delineated by the Box and Block Test (BBT) score as well as the presence of CP. The connections were then used as inputs in the estimation process. We used both multiple linear regression and artificial intelligence techniques for the prediction of motor outcome prognosis. The patients were also divided into two groups based on the side of their lesion (left or right hemisphere) in order to study the impact of stroke laterality on the motor outcome.

Materials and Methods

Subjects

The participants in this study belonged to a cross-sectional analysis at age 7 years of the AVCnn database (Accident Vasculaire Cérébral du nouveau-né, i.e., neonatal stroke; PHRC régional n°03-08052 and PHRC interrégional n°10-08026; Eudract number 2010-A00329-30). This cohort was described in detail elsewhere.[6,8] In a few words, 100 term newborns with an arterial cerebral infarct, confirmed by early brain imaging (CT and/or MRI before 28 days of life), who were symptomatic during the neonatal period (thus matching the 2007 definition of NAIS[6]) were consecutively enrolled between November 2003 and October 2006 from 39 French centers. Seventy-two children took part in a clinical, neuropsychological, and language assessment at 7 years (AVCnn[7ans]). During this assessment, an MRI was proposed to the families. Fifty-two children participated in this MRI study (AVCnn[signal]; PHRC 2010-07; Eudract number 2010-A00976-33). Among them, 38 had a

unilateral lesion in the median cerebral arterial (MCA) territory. However, after further examination six patients were excluded due to poor segmentation results (for more details please refer to (Dinomais et al., 2015a)), leaving 32 patients. They constituted the patient population of this study.

Based on a previous study that indicates different outcomes following the side of the lesion,[31] Patients were divided into two groups: patients with lesions in the left hemisphere (LLP) and patients with lesions in the right hemisphere (RLP). In addition to the LLP and RLP patients, we recruited 30 healthy controls (HC). These controls were matched in age and gender with the patients.[8] General characteristics of the participants are presented in Table 1 and a detailed description of the patients is presented in Supplementary Table A.

Informed written consent respecting the declaration of Helsinki was obtained from all participants/parents as well as approval from the ethical committee of the university hospital of Angers, France. Handedness was determined according to the Edinburgh inventory.[32]

Manual dexterity of contra- and ipsilesional hands

The motor performance of the ipsi- and contralesional hands of all NAIS patients were assessed using the Box and Block Tests (BBT). The BBT is an approved tool for measuring gross manual dexterity in children.[33] It consists of a box with two compartments separated in the middle. At the beginning, 100 small blocks are located in one of the compartments, on the same side of the tested hand. Children move as many cubes as they can from one compartment to the other. Both hands were evaluated. The individual score was obtained by counting the maximum number of cubes transferred by the ipsi- and contralesional hand in 1 min, thus the higher, the better.

Cerebral palsy

The evaluation team included either a pediatric neurologist or a pediatric physical and rehabilitation medicine practitioner experienced in children's disability. The definition given by the Surveillance for CP in Europe was used: permanent abnormal tone or decreased strength as a consequence of a nonprogressive early brain injury (present by definition in our population), and associated with a patent functional deficit.[34]

MRI acquisition and processing

Acquisition

Images were acquired on a 3.0 Tesla scanner (MAGNETOM Trio Tim system, Siemens, Erlangen, Germany, 12 channel head coil) at Neurospin, CEA-Saclay, France. Two Imaging sequences were collected for each participant.

The first was a high-resolution 3D T1-weighted volume using a magnetization-prepared rapid acquisition gradient-echo sequence [176 slices, repetition time (TR) 2300 msec, echo time (TE) 4.18 msec, field of view (FOV) 256 mm, flip angle = 9°, voxel size $1 \times 1 \times 1$ mm^3].

The second was a diffusion-weighted dual SE-EPI sequence with 30 diffusion encoding directions and a diffusion-weighting of $b = 1000$ s/mm^2 (TR = 9500 msec, TE = 86 msec, 40 slices, voxel size $1.875 \times 1.875 \times 3$ mm^3).

Lesion masks

For each patient, the boundaries of the lesion were manually delineated on a slice by slice basis by two of the authors (MD, SG) that were blinded to the clinical information, especially motor function. This delineation was performed on the individual 3D T1 images to create a binary lesion mask using the MRIcron software

Table 1. General profile of the participants.

	HC Mean (±SD) or n (%)	LLP Mean (±SD) or n (%)	RLP Mean (±SD) or n (%)	P-value*
Number (n)	30	18	14	–
Age (years)	7.71 (±.54)	7.23 (±0.13)	7.28 (±0.20)	0.543
Gender	Males: 14 (47%) Females: 16 (53%)	Males: 10 (56%) Females: 8 (44%)	Males: 9 (64%) Females: 5 (36%)	0.376[a]
Right-handed	27 (90 %)	6 (33 %)	14 (100 %)	0.180[a]
Lesion size (mL)	–	32.45 (± 33.21)	38.16 (± 46.94)	0.859
TIV	1395.4 (± 110.01)	1307.0 (± 157.71)	1277.7 (± 98.30)	0.127

HC, Healthy Controls; LLP, Left Lesioned Patients; RLP, Right Lesioned Patients; TIV, Total intracranial volume.
[a]Chi-squared test
*P-values are obtained by one-way Kruskal–Wallis nonparametric ANOVA.

(http://www.mccauslandcenter.sc.edu/mricro).[35] In case of a main branch MCA stroke, the lateral border of the lesion mask was drawn along the inner border of the skull, comprising the whole porencephaly.[36]

DWI preprocessing and fiber tracking

The diffusion images were processed using MRtrix3 software (https://www.mrtrix3.com) running on Ubuntu 18.04.2 LTS machine. Preprocessing of DWI images included denoising,[37,38] unringing to remove Gibb's artifacts,[39] motion and distortion correction.[40] Fiber orientation distribution (FOD) was obtained using constrained spherical deconvolution (CSD).[41,42] The FODs were then corrected for the effects of residual intensity inhomogeneities using multitissue informed log-domain intensity normalization.[43] In order to create the whole-brain tractogram, a probabilistic algorithm that performs a second-order Integration over FOD was used.[44] The maximum angle between successive steps was set to 60 degrees and the cutoff value was fixed at 0.2. One million streamlines tractogram was obtained per subject. Finally, these streamlines were filtered into 200000 streamlines using Spherical-deconvolution Informed Filtering of Tractograms (SIFT) to reduce CSD-based bias in overestimation of longer tracks compared to shorter tracks.[45] The subject-specific proportionality coefficient μ defined by the SIFT model was computed for the intersubject comparison which will be discussed further on in this section. All the aforementioned steps were performed in the diffusion native space.

Brain parcellation

The first step of brain parcellation consisted of preprocessing of the T1-weighted images of all the subjects using the FreeSurfer suite, version 6.0.0 (https://surfer.nmr.mgh.harvard.edu/), on a single DELL workstation running ubuntu 16.04 LTS (Intel R Core TM i7-7820HQ CPU @ 2.9GHz × 8). Preprocessing steps included classification of the gray and white matters as well as segmentation of subcortical structures.

The atlas used for the Structural Connectivity (SC) analysis was that of Glasser et al.[46] This atlas divides the cortical gray matter into 180 atlas regions per hemisphere. Subsequently, using Freesurfer, we constructed the volumetric atlas-based parcellation images for each subject including the 180 × 2 grey matter regions as well as 19 subcortical regions based on the FreeSurfer segmentation (9 × 2 homologs consisting of cerebellum, thalamus, caudate, putamen, pallidum, hippocampus, amygdala, accumbens, and ventral Dorsal Caudate (DC) plus brainstem). Accordingly, the obtained parcellation image included 379 distinct atlas regions in total.

For the NAIS patients, explicit lesion masking was performed before the parcellation to minimize the impact of the lesion on the estimates.[47]

In order to compute the structural connectivity matrix, we registered the volumetric atlas-based parcellation images into the individual diffusion space of the corresponding subject using the FSL FLIRT suite (FMRIB's Linear Image Registration Tool, https://fsl.fmrib.ox.ac.uk/fsl/fslwiki/FLIRT). Then, using MRtrix, the atlas-based parcellation in diffusion space was overlayed onto the whole-brain tractogram which allowed us to identify the set of fibers F(i , j) connecting each pair of nodes representing the atlas regions i and j. The metric was collected in a 379 × 379 matrix defined as the connectivity matrix where each cell c(i, j) represents the number of streamlines connecting the areas i and j. The diagonal of the connectivity matrix was set to zero in order to discard the connections in the same atlas area.

However, we have to point out that this metric is highly dependent on the atlas region volume as well as the overall intracranial volume. Accordingly, for group comparisons, these matrices were normalized by the individual brain volume[30,48] and multiplied by the proportionality coefficient previously mentioned.[45]

The block diagram presenting an overview of the methodology used in order to obtain the structural connectivity matrix is depicted in Figure 1.

Motor connectivity mapping

In this work, we were interested in the impact of the NAIS on the motor outcome in particular. The cerebral areas responsible for motor performance and dexterity constituted the so-called brain motor system[46,49,50] and are presented in Table 2. Consequently, the 52 × 52 motor connectivity matrix, that reflects the connections between the motor areas, was extracted from the 379 × 379 structural connectivity matrix as depicted in Figure 2A. Afterward, in order to reduce the number of connections to analyze, to connections of interest, we computed the mean motor connectivity matrix of the control group and then we only kept the cells that were higher than 10% of the maximum connection value (Fig. 2B). In this manner, we only kept the main links that describe the connections between the motor areas. These links are divided into intra (LH⇔LH and RH⇔RH) and interhemisphere (LH⇔RH) connections and are presented in Table 3 and Figure 2C.

Statistical analysis

Statistical tests across groups were conducted using Matlab 2017a. For the comparison between healthy and
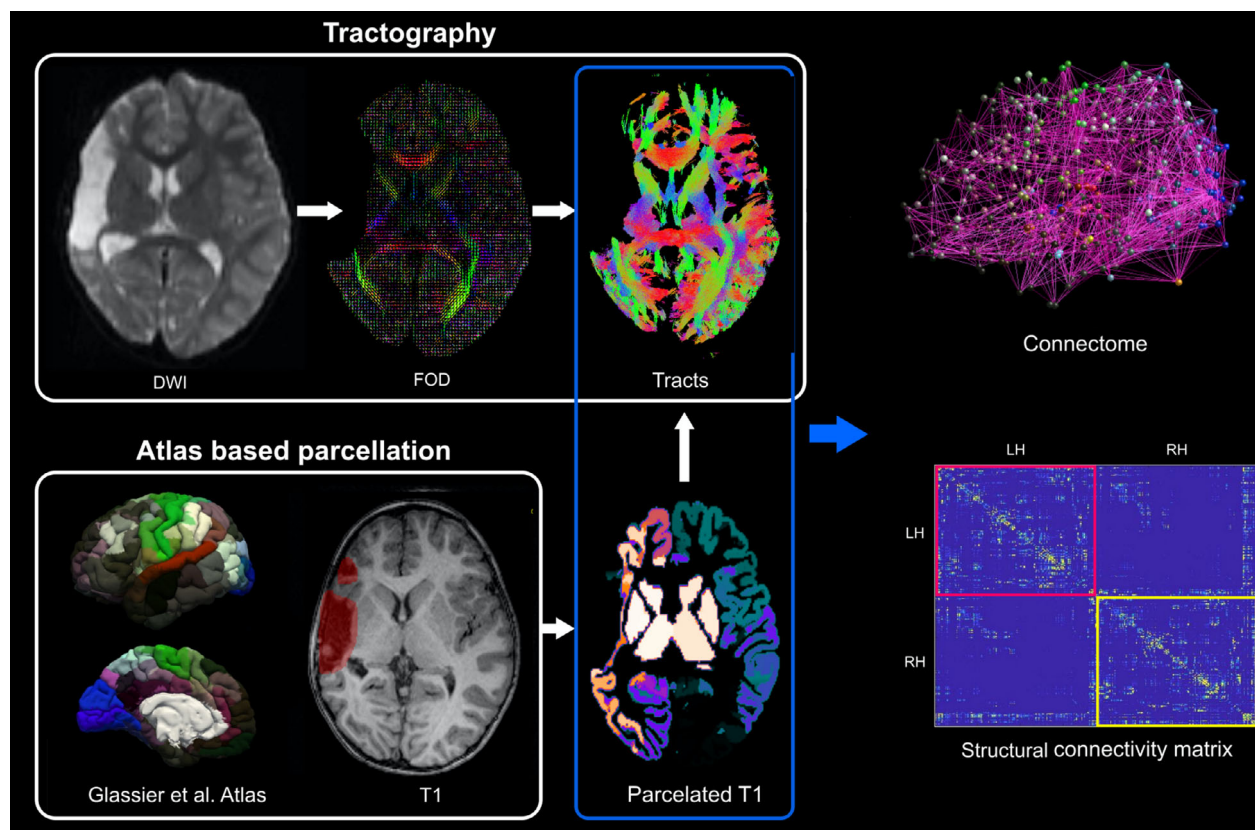
Figure 1. Overview of the methodology. The creation of the structural connectivity matrix consists of different steps. These steps include the processing of T1-weighted images (second row) with FreeSurfer and FSL as well as diffusion-weighted images with MRtrix3 (first row). The obtained connectivity matrix consists of 379 × 379 connections weights.

patient groups, the two-sample Kolmogorov–Smirnov test was used since the samples did not follow a normal distribution. We used Spearman's correlation coefficient to measure the linear correlation between the connectivity metric and the corresponding BBT score as well as the presence or not of CP. Comparisons between connection weights were performed for each score. Therefore, no multiple comparisons were performed in this study. All results with $P < 0.05$ were considered significant.

Estimation of motor outcome

MLR

To model the relationship between the brain connections of interest in the motor area and the motor performance, we used a multiple linear regression model (MLR). This model is used to estimate the BBT score of the contralesional (affected) hand from a group of structural connection scores chosen as links of interest (LOI)s. These LOIs were determined after a correlation analysis between the BBT scores and the motor SC scores or connectivity

metrics. The estimated MLR model can be presented by the following equation:

$$y = w_0 + w_1 x_1 + w_2 x_2 + \cdots + w_n x_n + \varepsilon.$$

Where y is the BBT score, x_i is the connection score of the ith connection of interest (the links that are significantly correlated with the BBT score), w_i is the slope coefficient of each x_i, w_0 is the constant offset term, ϵ is the error term, and n is the number of features (correlated links scores).

The accuracy of the estimation was computed following the leave-one-participant-out cross-validation technique. Accordingly, one patient was excluded, and the remaining patients were used for the training of the MLR model. Afterward, the model was evaluated by estimating the BBT score of the excluded patient using the model. This process was repeated so each time a different patient was excluded until all patients had a turn. The accuracy is then evaluated by computing the estimation error percentage between the real and estimated values of BBT.

Table 2. The motor cortical areas and corresponding subareas used for the motor connectivity mapping. The abbreviations used are the same as in (Glasser et al., 2016).

Motor areas and sub-areas	
Primary motor cortex (M1)	Cingulate cortex (CC)
	Dorsal part of 24d (24dd)
	Ventral part of 24d (24dv)
Primary somatosensory cortex (S1)	Parietal cortex (PC)
BA3a Fundus of the central sulcus	Medial Area 7P (7 Pm)
BA3b posterior bank of the sulcus	Medial BA 7 (7m)
BA1	Lateral area 7A (7AL)
BA2	Medial Area of 7A (7Am)
	Lateral part of Area 7P (7 PL)
	7 PC
Secondary somatosensory cortex (S2)	Supplementary (SMA)
Posterior part of Brodmann's 43 (OP4)	Lateral BA6 (6ma)
Frontal OPercular area (PFOP)	Posterior BA6 (6mp)
	Supplementary and cingulate eye fields (SCEF)
Premotor cortex (PMC)	Thalamus
Anterior part of BA6 (6a)	Cerebellum
ventral part of BA6(6v)	
Rostral part of BA6 (6r)	
Area bounded by FEF and PEF (55b)	
Frontal Eye Field (FEF)	
PreFrontal Eye Field (PEF)	

BA, Brodmann Area.

KNN

To predict the presence or not of CP, a K-Nearest Neighbor KNN classification model was employed using Matlab 2015a.[51] Two nearest neighbors, corresponding to either no CP (0) or CP (1), were set for the classifier. For each group of patients (LLP and RLP), motor connectivity values were used as features in order to train the KNN model. The accuracy of the prediction was evaluated using also the leave-one-participant-out cross-validation technique. The accuracy was then computed as the percentage of correctly classified patients (that were not a part of the training set) between CP or no CP.

Results

Group comparisons

Tables 4 and 5 present the motor area connections that are significantly different from the controls in the LLP and RLP groups. The results of the statistical comparisons are illustrated in Figure 3 for the global motor areas previously defined in Table 2. The Main intrahemisphere disconnections in the lesioned hemisphere for the LLP group are between M1 and S1, PMC subareas as well as between Thalamus and SMA subareas (see Table 3,

Fig. 3). This is expected due to the location of the lesions near the M1 and S1 in the left hemisphere for the LLP group (please refer to Fig. S1). Then as well, a mirroring disconnection pattern was observed in the contralesioned hemisphere (RH) for the LLP group. This was observed as a significantly lower connectivity between M1 and S1. There was also a disconnection between S1 and Thalamus (Table 3, Fig. 3). Regarding interhemisphere connections, no significant disconnections were observed for the LLP compared to the healthy control group.

LLP and Controls group comparison also revealed higher connectivity scores between the thalamus and the S1 (Table 3) in the lesioned hemisphere in addition to increased connection between M1 and SMA of the contra-lesioned hemisphere. But more importantly, increase in interhemispheric connections was observed between the left and right thalamus and cerebellum and between the left CC and right SMA.

Similar results were depicted for the RLP group as displayed in Table 5. Primary disconnections in the lesioned hemisphere (RH) were found between M1 and PMC as well as between S1 and thalamus (See Table 5, Fig. 3). Similar to the LLP group, the contra-lesioned hemisphere of the RLP patients exhibited a decrease in the connection scores between motor areas equivalent to the ones observed in the lesioned hemisphere (Table 5, Fig. 3). RLP patients also demonstrated higher connections than controls in the lesioned hemisphere between S1 and thalamus and in the contralesional hemisphere between M1 and cerebellum. Furthermore, interconnections between the left and right thalamus were found to be greater than in the control group.

BBT score correlation analysis and prediction

In order to identify the connections that are correlated with the motor outcome for both LLP and RLP groups, we computed the linear correlation between the BBT score and all the motor area connections scores of the corresponding hemisphere. Table 6 displays the intrahemisphere connections that are linearly correlated with the contralesional and ipsilesional hands BBT scores for the LLP and RLP groups. In the case of LLP group, the contralesional hand BBT score was found to be positively correlated with the ipsilesional connectivity weight between the thalamus and PC and negatively correlated with the connectivity weight between the left and right cerebellum. For the In ipsilesional hand BBT score, a negative correlation was found with the contralesional connection weight between the M1 and thalamus as well as positive correlations between the M1 and the cerebellum and between the thalamus and the cerebellum. In
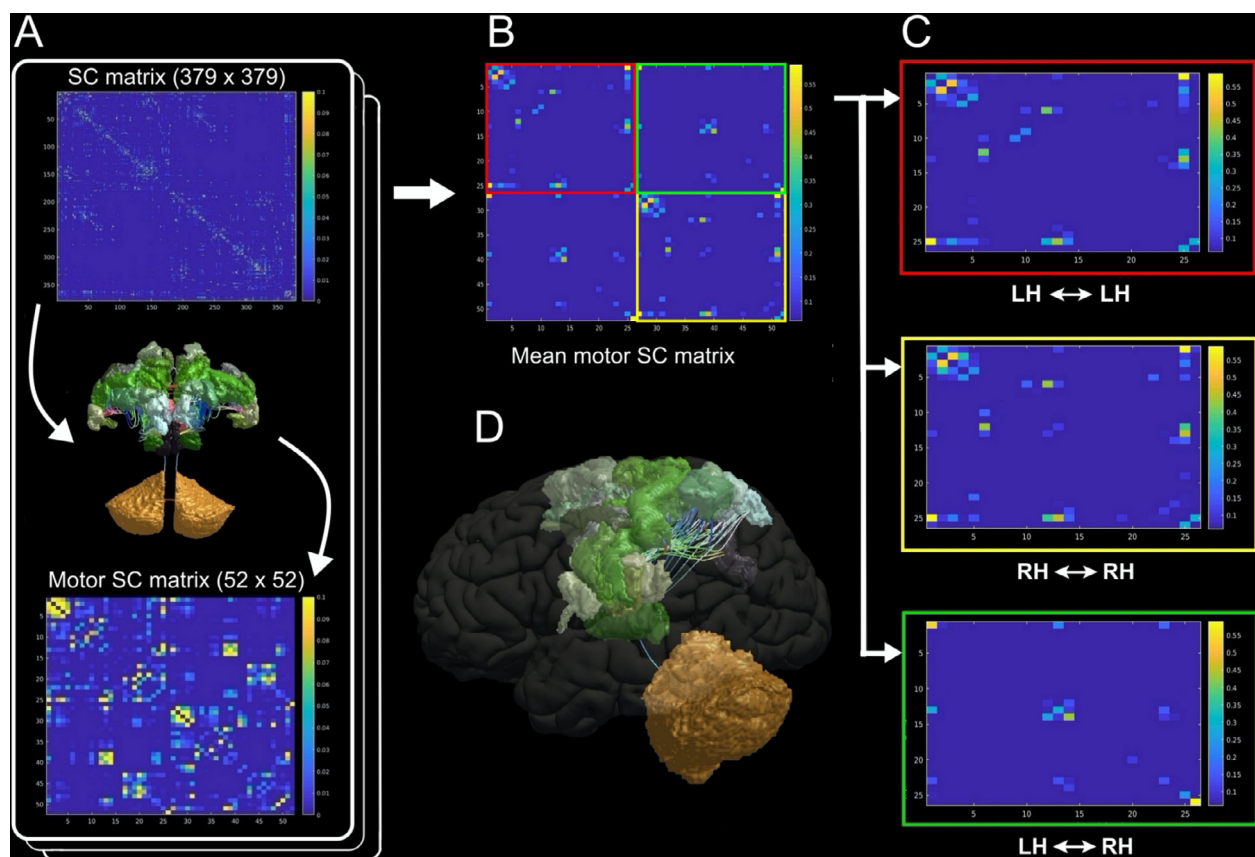
Figure 2. General process of connection selection. (A) Extracting the motor SC matrix from the whole brain 379 × 379 matrix. With 24 motor areas in each hemisphere 52 nodes were obtained. (B) The mean motor SC for the control group. (C) The connections of interest were chosen for this study. (D) Illustration of the motor connectome for the left hemisphere.

addition, a negative correlation with the interhemispheric cerebellum connections were found.

For the RLP group, we found a negative correlation of the contralesional BBT with the S1 and M1 as well as M1 and thalamus connectivity weights of the ipsilesional hemisphere and a positive correlation with the connections between the left SMA and right CC. For the ipsilesional BBT, no significant correlations were depicted with the connectivity scores.

The prediction accuracy following the leave-one-participant-out cross-validation technique of the BBT score based on the connections of interest identified in Table 6 for each group and each hand is depicted in Table 7. The accuracy was tested by using either the most significantly correlated, or all connections that were found to be significantly correlated with the BBT score. These connexions are depicted in Table 6. The results highlight a similar prediction BBT score for both groups with a slightly better performance when combining all the connectivity scores compared to only the most significant one.

CP correlation analysis and prediction

Finally, with regard to the presence or not of CP, one connection of interest was identified for each group. These connections were between the SMA (supplementary and cingulate eye fields) and thalamus of the non lesioned hemisphere for the LLP group and between the left SMA and right CC for the RLP. The connectivity score associated with these regions exhibited a significantly positive point biserial correlation with the absence of CP. Using these specific connection scores we were able to deliver a good classification accuracy for both groups (please refer to Table 8).

Discussion

In this work, we used fiber tractography and high-resolution connectomics in order to evaluate the relationship between specific disconnections between motor areas and motor outcome at age 7 following neonatal stroke. One of the main findings is that disconnections observed in the contralesional hemisphere mimics those found in lesioned

Table 3. The intra and interhemisphere links used in the motor function connectivity analysis.

Intrahemisphere connections	Interhemispheric connections
1 → M1 ⇔ BA 3a	1 → M1 LH ⇔ M1 RH
2 → M1 ⇔ BA 3b	2 → M1 LH ⇔ 6mp RH
3 → M1 ⇔ BA 1	3 → M1 LH ⇔ 24dd RH
4 → M1 ⇔ 6V	4 → M1 LH ⇔ thalamus RH
5 → M1 ⇔ 6mp	5 → 6ma LH ⇔ 6ma RH
6 → M1 ⇔ thalamus	6 → 6ma LH ⇔ 6mp RH
7 → M1 ⇔ cerebellum	7 → 6ma LH ⇔ SCEF RH
8 → BA3a ⇔ BA3b	8 → 6mp LH ⇔ M1 RH
9 → BA3a ⇔ BA1	9 → 6mp LH ⇔ 6mp RH
10 → BA3a ⇔ BA2	10 → 6mp LH ⇔ SCEF RH
11 → BA3a ⇔ thalamus	11 → 6mp LH ⇔ 24dd RH
12 → BA3b ⇔ BA1	12 → SCEF LH ⇔ 6ma RH
13 → BA3b ⇔ BA2	13 → SCEF LH ⇔ 6mp RH
14 → BA3b ⇔ thalamus	14 → SCEF LH ⇔ SCEF RH
15 → BA1 ⇔ BA2	15 → SCEF LH ⇔ 24dd RH
16 → BA1 ⇔ thalamus	16 → SCEF LH ⇔ 24dv RH
17 → BA2 ⇔ 7AL	17 → 7Am LH ⇔ 7Am RH
18 → BA2 ⇔ 7PC	18 → 24dd LH ⇔ M1 RH
19 → BA2 ⇔ thalamus	19 → 24dd LH ⇔ 6mp RH
20 → 6a ⇔ FEF	20 → 24dd LH ⇔ SCEF RH
21 → 6a ⇔ 6ma	21 → 24dd LH ⇔ 24dd RH
22 → 6a ⇔ 6mp	22 → 24dv LH ⇔ SCEF RH
23 → 6a ⇔ thalamus	23 → Thalamus LH ⇔ thalamus RH
24 → 55b ⇔ FEF	24 → cerebellum LH ⇔ cerebellum RH
25 → 6ma ⇔ 6mp	
26 → 6ma ⇔ thalamus	
27 → 6mp ⇔ 24dd	
28 → 6mp ⇔ thalamus	
29 → SCEF ⇔ 24 dv	
30 → SCEF ⇔ thalamus	
31 → 7AL ⇔ thalamus	
32 → 24dd ⇔ thalamus	
33 → 24dd ⇔ 24dv	
34 → Thalamus ⇔ cerebellum	

hemispheres in both LLP and RLP groups near the lesion area (please refer to Fig. S1). This shows that even though there is no lesion (by definition) in the contralesional ("healthy") hemisphere, still it suffers from the neonatal stroke consequences, with a decreased connectivity between regions similar to those found in the lesioned hemisphere compared to healthy controls. These regions are mainly within and between S1 and M1 (close to the lesion site) as well as between S1, M1 and thalamus, PMC, respectively. This can be seen as a direct result of the stroke infarct where the disconnections in the thalamus are reflected in a decreased connectivity through the feed-forward processing function.[52] These results are consistent with other studies that underlined the importance of the contralesional hemisphere in motor and sensorimotor network development or reorganization following both early unilateral stroke[22,23] and adult stroke.[53]

Another important finding in this study is that higher connectivity weights were found in patient groups compared to healthy controls. This higher connectivity was observed both in interhemispheric and intrahemispheric connections. The interhemispheric connectivity increase was found between the ipsilesional thalamus and S1 for both groups and between the contralesional M1 and cerebellum/SMA (RLP/LLP). In the case of interhemispheric connections, stronger connections were observed between the left and right thalamus for both groups and between the left and right cerebellum for the LLP group. This increased intrahemispheric connectivity in particular regions in both groups, even though not exactly the same, could portray a compensatory phenomenon in the lesioned hemisphere wherein the thalamus plays a major role in motor plasticity and is a major hub for the motor system.[53] It has been demonstrated that remaining neurons in the peri-infarct cortex go through a structural remodeling that is linked with a remapping of lost functions.[54] Therefore, it is conceivable that the increase in the aforementioned connectivity can be a form of (re)organization phenomenon.[23] This is consistent with the recent work of Jang et al.[55] where they found an increased thalamocortical between the lesioned and contralesional hemispheres in the case of a stroke patient. This result is particularly important in the case of NAIS given the fact that thalamocortical network connectivity is altered during brain maturation[56,57] and decreased connectivity was linked to motor impairments.[58]

Moreover, in the LLP group, an increase in the interhemisphere connections was observed between the contralesional SMA and the ipsilesional CC (Table 4). This can be seen as a compensatory mechanism to the disconnections mentioned earlier. However, this is only speculative. Giving another explanation on why we found increased connectivity in some particular regions (regions depending on the side of the infarct) in our patients is not a trivial task.

Correlation analysis between the BBT score and the connectivity score revealed valuable input about the motor outcome following NAIS. We found a significant positive correlation between the contralesional hand motor score and ipsilesional connections in the LLP group (Tables 4 and 6). These fibers connect the thalamus and the PC, indicating that a higher score is directly linked to the amount of compensatory fibers between the thalamus and PC following the stroke. Concerning the negative correlation found between the contralesional BBT score and the interhemispheric connectivity weight between the cerebellums, it can demonstrate the role of these regions in motor inhibitory system,[59–61] which is dominant in the right hemisphere.[62] In other terms, our results support the fact that higher connectivity in regions

Table 4. The significant difference results of the structural connectivity strength comparison between controls and LLP groups.

	Controls > LLP			Controls < LLP		
	Area	Subsection	P-value	Area	Subsection	P-value
Intra LH (ipsi)	M1 ⇔ S1	M1 ⇔ BA1	0.00706	S1 ⇔ Thalamus	BA2 ⇔ Thalamus	0.0261
	M1 ⇔ PMC	M1 ⇔ 6V	0.0030			
	Thalamus ⇔ SMA	Thalamus ⇔ 6ma	0.0375			
Intra RH (contra)	M1 ⇔ S1	M1 ⇔ BA3a	0.0070	M1 ⇔ SMA	M1 ⇔ 6mp	0.0329
	S1 ⇔ Thalamus	BA1 ⇔ Thalamus	0.0279			
Inter H				LH CC ⇔ RH SMA	LH 24dd ⇔ RH SCEF	0.0129
				LH Cerebellum ⇔ RH Cerebellum	LH Cerebellum ⇔ RH Cerebellum	0.0129
				LH Thalamus ⇔ RH Thalamus	LH Thalamus ⇔ RH Thalamus	0.0178

Table 5. The significant difference results of the structural connectivity metric comparison between controls and RLP groups.

	Controls > RLP			Controls < RLP		
	Area	Subsection	P-value	Area	Subsection	P-value
Intra RH (ipsi)	M1 ⇔ PMC	M1 ⇔ 6V	0.0470	S1 ⇔ Thalamus	BA3a ⇔ Thalamus	0.0317
	S1 ⇔ Thalamus	BA1 ⇔ Thalamus	0.0161			
Intra LH (contra)	M1 ⇔ S1	M1 ⇔ BA1	0.0028	M1 ⇔ Cerebellum	M1 ⇔ Cerebellum	0.0436
	M1 ⇔ Thalamus	M1 ⇔ Thalamus	0.0038			
	S1 ⇔ Thalamus	BA3a ⇔ Thalamus	0.0047			
		BA1 ⇔ Thalamus	0.0228			
		BA2 ⇔ Thalamus	0.0077			
Inter H				LH Thalamus ⇔ RH Thalamus	LH Thalamus ⇔ RH Thalamus	0.0248

playing a role in inhibitory systems, could be accompanied by poorer motor performance. For the ipsilesional BBT score, the positive correlations were for the connections between the thalamus and cerebellum as well as between the M1 and the cerebellum in the contralesional hemisphere. The negative correlations were found between M1 and the thalamus. The importance of the thalamus in predicting hand motor function has been already discussed many times.[63,64] These results indicate that the thalamus connections with other motor regions are directly linked to the motor score as it was demonstrated recently by.[65]

In the RLP group, correlation analysis showed a linear positive correlation between the contralateral hand BBT score and the ipsilesional intrahemispheric connectivity weights between M1 and S1 as well as between S1 and the thalamus which were found lower than in the control group. For the ipsilesional hand BBT score, we did not find significant correlations with the connectivity scores. This can be explained by the low standard deviation between ipsilesional and contralesional BBT scores for the RLP groups as well as the low number of patients. Using the connections of interest, we were able to estimate the BBT score with good enough accuracy.

Finally, we computed the point biserial correlation between the connectivity weight and the CP presence/ absence. We only found one connection of interest for each group of patients. This connection concerned the thalamus, SMA, and CC confirming their central role in motricity following a brain lesion. Based solely on these connection weights, we were able to classify the patients with regard to the presence/absence of CP with good accuracy. This highlights the direct link between the weight of these structural connections and the presence of CP. Our results confirm that the presence of CP is associated with higher structural connectivity in the contralesional ("healthy") hemisphere after unilateral early brain lesion. This is consistent with studies that showed that SMA and CC regions are altered in children with CP.[66] Another explanation could be the reorganization hypothesis that can occur in some cases after a unilateral brain lesion where the contralesional hemisphere takes over some of the motor control relative to the affected extremities.[67]

To conclude this discussion, we have to mention some of the limitations of this work. The main limitation of this study was the absence of the BBT score for the control group which would have provided an extra layer for our correlation analysis and validated our results. Another limitation would be the limited sample number for the patients especially after dividing them into two unequal groups (LLP and RLP), however, our cohort are very
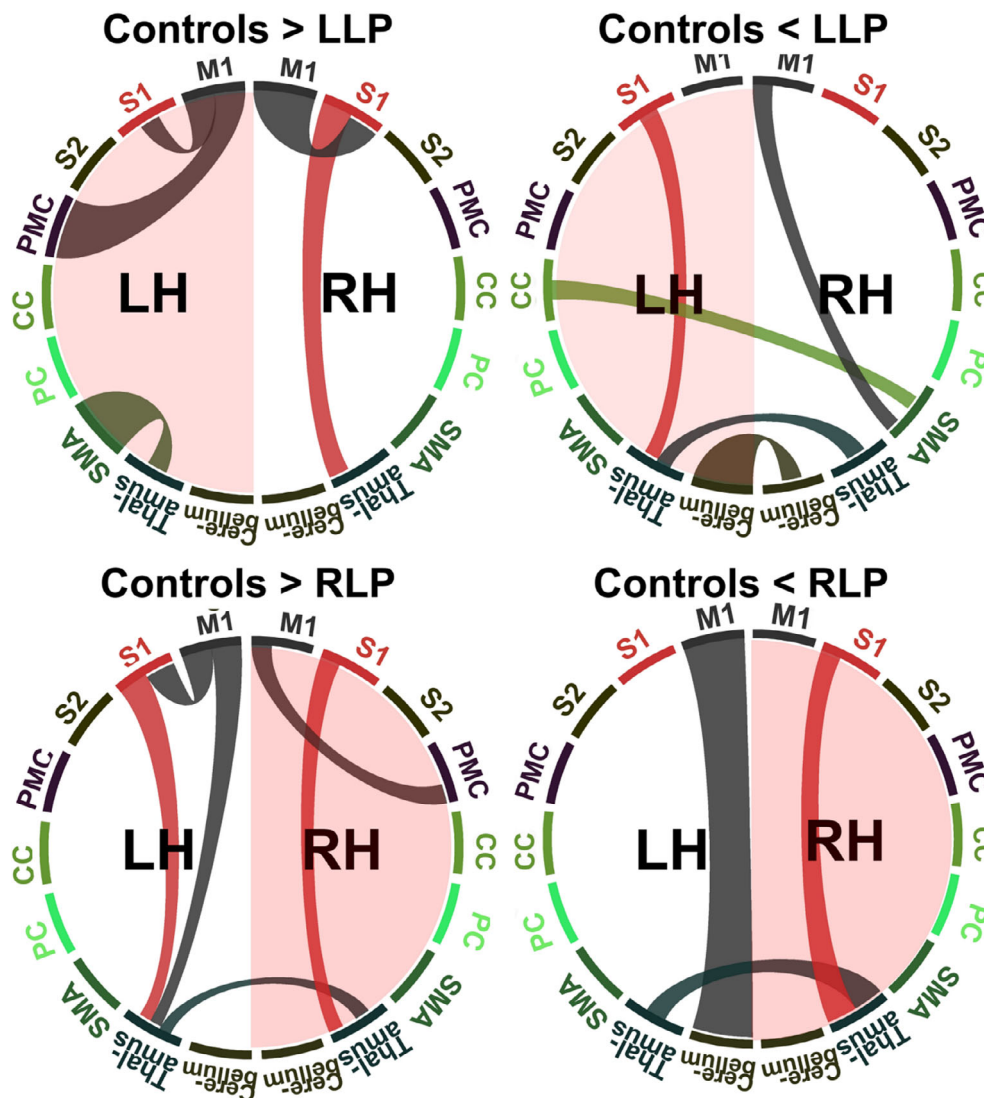
Figure 3. Circular representation of the significantly different structural connectivity tracts between patients (LLP and RLP) and controls for the different motor areas defined in Table 2.

homogenous in terms of age at the evaluation and type of lesion (neonatal stroke is "presented as the ideal human model of developmental neuroplasticity"[68]). Moreover, we found it very important based on the asymmetric nature of the brain both in connectivity and morphology.[69,70] However, we did do the same methodology by flipping the brain of the RLP group and combining the LLP and RLP groups into one NAIS group. The connectivity score comparisons between controls and NAIS patients as well as the BBT score correlation with the connectivity weights are presented in supplementary Tables 1 and 2, respectively. These results furthermore approve our choice to divide patients based on the lesion side since it allows for less ambiguities and more accurate conclusions. Lastly, we

have to note that every neuroimaging method has its limitations and tractography is no exception especially in the lesioned brain. New fixel-based analysis techniques can help to better process the lesioned brain. Future work will include whole-brain fixel-based analysis of the NAIS brain in order to confirm the results introduced in this article.

Conclusions

This study underlines the importance of tracts inspection in addition to other techniques (lesion mapping, morphometry analysis) in estimating motor outcome and "recovery" following neonatal stroke. We demonstrated that cortical regions in the ipsilesional as well as contralesional

Table 6. The motor connections that are linearly correlated with the BBT in the case of the LLP and RLP groups.

		Areas	Subsections	R	P-value
LLP	Contralesional BBT	LH PC ⇔ LH Thalamus	LH 7AL ⇔ LH Thalamus	0.5690	0.0100
		LH Cerebellum ⇔ RH Cerebellum	LH Cerebellum ⇔ RH Cerebellum	-0.5972	0.0089
	Ipsilesional BBT	RH M1 ⇔ RH Thalamus	RH M1 ⇔ RH Thalamus	-0.5415	0.0203
		RH M1 ⇔ RH Cerebellum	RH M1 ⇔ RH Cerebellum	0.5379	0.0213
		RH Thalamus ⇔ RH Cerebellum	RH Thalamus ⇔ RH Cerebellum	0.4732	0.0473
		LH Cerebellum ⇔ RH Cerebellum	LH Cerebellum ⇔ RH Cerebellum	-0.5395	0.0209
RLP	Contralesional BBT	RH M1 ⇔ RH S1	RH M1 ⇔ RH BA3a	-0.6865	0.0067
		LH SMA ⇔ RH CC	LH SCEF ⇔ RH 24dd	0.5598	0.0374
	Ipsilesional BBT	–	–	–	–

Table 7. The Accuracy of predicting BBT scores using multiple linear regression models with leave-one-participant out cross-validation using either all or the most significantly correlated connection weight to the corresponding BBT score. The most significant connectivity scores are presented in Table 6 (red).

	BBT	Linear regression model		Connections	Prediction accuracy
LLP	Contralesional	$y \sim w0+w_1x_1$	$w_0 = 33.135$ $w_1 = -64408$	1- LH Cerebellum ⇔ RH Cerebellum	71.45%
		$y \sim w0+w_1x_1 + w_2x_2$	$w_0 = 27.064$ $w_1 = -50481$ $w_2 = 4729.1$	1- LH Cerebellum ⇔ RH Cerebellum 2- LH 7AL ⇔ LH Thalamus	78.4%
	Ipsilesional	$y \sim w0+w_1x_1$	$w_0 = 38.193$ $w_1 = -4006.6$	1- RH M1 ⇔ RH Thalamus	84.01%
		$y \sim w0+w_1x_1 + w_2x_2+w_3x_3 + w_4x_4$	$w0 = 37.043$ $w1=-3759.4$ $w2 = 5400.8$ $w3 = 48864$ $w4=-23470$	1- RH M1 ⇔ RH Thalamus 2- RH M1 ⇔ RH Cerebellum 3- RH Thalamus ⇔ RH Cerebellum 4- LH Cerebellum ⇔ RH Cerebellum	87.14%
RLP	Contralesional	$y \sim w0+w_1x_1$	$w0 = 39.13$ $w1=-1203.1$	1-RH M1 ⇔ RH BA3a	87.30%
		$y \sim w0+w_1x_1 + w_2x_2$	$w_0 = 32.183$ $w_1=-965.68$ $w_2 = 51785$	1-RH M1 ⇔ RH BA3a 2-LH SCEF ⇔ RH 24dd	89.12%
	Ipsilesional	–	–	–	–

Table 8. The motor connections that are correlated with the CP presence/absence and the results of the classification of patients between CP and non-CP using these connections.

	Connection	Correlation value	P-value	Classification accuracy
LLP	RH SMA(6mp) ⇔ RH thalamus	−0.5016	0.0287	94.73%
RLP	LH SMA (SCEF) ⇔ RH thalamus	−0.6143	0.0194	92.85%

hemispheres exhibit a reduction in connectivity when compared to healthy controls suggesting that cortical areas directly unaffected by the stroke still exhibit fiber losses. Neonatal stroke does not appear to be only a focal lesion but a lesion that impacts the whole developing brain. We also found an increase in connections portraying some sort of compensatory mechanism in motor areas that could be explained by a structural (re)organization scheme. Finally, we were able to estimate motor outcome assessed by BBT scores and CP presence based on connections weights that were linearly correlated with them. We highlighted the importance of the preservation of the connectivity to and from the thalamus. Future work could include a combination of structural analysis with functional connectivity analyses during resting state, which could add further insight into the neonatal stroke impact of different outcomes.

Conflict of Interest

None declared.

References

1. Dunbar M, Kirton A. Perinatal stroke: mechanisms, management, and outcomes of early cerebrovascular brain injury. Lancet Child Adolesc Health 2018;2:666–676.

2. Raju TNK, Nelson KB, Ferriero D, Lynch JK. Ischemic perinatal stroke: summary of a workshop sponsored by the National Institute of Child Health and Human Development and the National Institute of Neurological Disorders and Stroke. Pediatrics 2007;120:609–616.

3. Fluss J, Dinomais M, Chabrier S. Perinatal stroke syndromes: similarities and diversities in aetiology, outcome and management. Eur J Paediatr Neurol 2019;23:368–383.

4. Kirton A, deVeber G. Paediatric stroke: pressing issues and promising directions. Lancet Neurol 2015;14:92–102.

5. Kirton A, deVeber G. Life after perinatal stroke. Stroke 2013;44:3265–3271.

6. Chabrier S, Peyric E, Drutel L, et al. Multimodal outcome at 7 years of age after neonatal arterial ischemic stroke. J Pediatr 2016;172:156–161.e3.

7. Husson B, Hertz-Pannier L, Renaud C, et al. Motor outcomes after neonatal arterial ischemic stroke related to early MRI data in a Prospective Study. Pediatrics 2010;126: e912–e918.

8. Dinomais M, Hertz-Pannier L, Groeschel S, et al. Long term motor function after neonatal stroke: lesion localization above all. Hum Brain Mapp 2015;36:4793–4807.

9. Jang SH. Prediction of motor outcome for hemiparetic stroke patients using diffusion tensor imaging: a review. NeuroRehabilitation 2010;27:367–372.

10. Song J, Nair VA, Young BM, et al. DTI measures track and predict motor function outcomes in stroke rehabilitation utilizing BCI technology. Front Hum Neurosci 2015;9:195.

11. Feng W, Wang J, Chhatbar PY, et al. Corticospinal tract lesion load: an imaging biomarker for stroke motor outcomes. Ann Neurol 2015;78:860–870.

12. Yoo YJ, Kim JW, Kim JS. Corticospinal tract integrity and long-term hand function prognosis in patients with stroke. Front Neurol 2019;10:374.

13. Lam TK, Binns MA, Honjo K, et al. Variability in stroke motor outcome is explained by structural and functional integrity of the motor system. Sci Rep 2018;8:1–11.

14. Lin LY, Ramsey L, Metcalf NV, et al. Stronger prediction of motor recovery and outcome post-stroke by cortico-spinal tract integrity than functional connectivity [Internet]. PLoS One 2018;13:e0202504. Available from: https://www.ncbi.nlm.nih.gov/pmc/articles/PMC6107181/

15. Wiedemann A, Pastore-Wapp M, Slavova N, et al. Impact of stroke volume on motor outcome in neonatal arterial ischemic stroke. Eur J Paediatr Neurol 2020;25:97–105.

16. Mackay MT, Slavova N, Pastore-Wapp M, et al. Pediatric ASPECTS predicts outcomes following acute symptomatic neonatal arterial stroke. Neurology 2020;94:e1259–e1270.

17. Grefkes C, Fink GR. Connectivity-based approaches in stroke and recovery of function. Lancet Neurol 2014;13:206–216.

18. Grefkes C, Fink GR. Reorganization of cerebral networks after stroke: new insights from neuroimaging with connectivity approaches. Brain 2011;134:1264–1276.

19. Hensel L, Tscherpel C, Freytag J, et al. Connectivity-related roles of contralesional brain regions for motor performance early after stroke. Cereb Cortex. 2020. https://doi.org/10.1093/cercor/bhaa270

20. Desowska A, Turner DL. Dynamics of brain connectivity after stroke. Rev Neurosci 2019;30:605–623.

21. Carter AR, Shulman GL, Corbetta M. Why use a connectivity-based approach to study stroke and recovery of function? NeuroImage 2012;62:2271–2280.

22. Saunders J, Carlson HL, Cortese F, et al. Imaging functional motor connectivity in hemiparetic children with perinatal stroke. Hum Brain Mapp 2019;40:1632–1642.

23. Woodward KE, Carlson HL, Kuczynski A, et al. Sensory-motor network functional connectivity in children with unilateral cerebral palsy secondary to perinatal stroke. NeuroImage 2019;21:101670.

24. Carlson HL, Sugden C, Brooks BL, Kirton A. Functional connectivity of language networks after perinatal stroke. NeuroImage 2019;23:101861

25. Kornfeld S, Yuan R, Biswal BB, et al. Resting-state connectivity and executive functions after pediatric arterial ischemic stroke. NeuroImage 2018;17: 359–367.

26. Taylor PN, Wang Y, Kaiser M. Within brain area tractography suggests local modularity using high resolution connectomics. Sci Rep 2017;7:1–9.

27. Taylor PN, Kaiser M, Dauwels J. Structural connectivity based whole brain modelling in epilepsy. J Neurosci Methods 2014;236:51–57.

28. Lim S, Han CE, Uhlhaas PJ, Kaiser M. Preferential detachment during human brain development: age- and sex-specific structural connectivity in Diffusion Tensor Imaging (DTI) Data. Cereb Cortex 2015;25:1477–1489.

29. Leonardo B, Chris R, Julius F. Assessing the clinical effect of residual cortical disconnection after ischemic strokes. Stroke 2014;45:988–993.

30. Yourganov G, Fridriksson J, Rorden C, et al. Multivariate connectome-based symptom mapping in post-stroke patients: networks supporting language and speech. J Neurosci 2016;36:6668–6679.

31. Harrach MA, Rousseau F, Groeschel S, et al. Alterations in cortical morphology after neonatal stroke: compensation in the contralesional hemisphere? Dev Neurobiol 2019;79:303–316.

32. Oldfield RC. The assessment and analysis of handedness: the Edinburgh inventory. Neuropsychologia 1971;9:97–113.

33. Mathiowetz V, Volland G, Kashman N, Weber K. Adult norms for the box and block test of manual dexterity. Am J Occup Ther 1985;39:386–391.

34. Cans C, Dolk H, Platt M, et al. Recommendations from the SCPE collaborative group for defining and classifying cerebral palsy. Dev Med Child Neurol 2007;49 (s109):35–38.

35. Rorden C, Karnath H-O, Bonilha L. Improving Lesion-symptom mapping. J Cogn Neurosci 2007;19:1081–1088.

36. Dinomais M, Hertz-Pannier L, Groeschel S, et al. Does contralesional hand function after neonatal stroke only depend on lesion characteristics? Stroke 2016;47:1647–1650.

37. Veraart J, Novikov DS, Christiaens D, et al. Denoising of diffusion MRI using random matrix theory. NeuroImage 2016;142:394–406.

38. Veraart J, Fieremans E, Novikov DS. Diffusion MRI noise mapping using random matrix theory. Magn Reson Med 2016;76:1582–1593.

39. Kellner E, Dhital B, Kiselev VG, Reisert M. Gibbs-ringing artifact removal based on local subvoxel-shifts. Magn Reson Med 2016;76:1574–1581.

40. Andersson JLR, Sotiropoulos SN. An integrated approach to correction for off-resonance effects and subject movement in diffusion MR imaging. NeuroImage 2016;125:1063–1078.

41. Tournier J-D, Calamante F, Gadian DG, Connelly A. Direct estimation of the fiber orientation density function from diffusion-weighted MRI data using spherical deconvolution. NeuroImage 2004;23:1176–1185.

42. Tournier J-D, Calamante F, Connelly A. Robust determination of the fibre orientation distribution in diffusion MRI: non-negativity constrained super-resolved spherical deconvolution. NeuroImage 2007;35:1459–1472.

43. Raffelt D, Dhollander T, Tournier J-D, et al. Bias field correction and intensity normalisation for quantitative analysis of apparent fibre density. 2017.

44. Tournier J-D, Calamante F, Connelly A. Improved probabilistic streamlines tractography by 2nd order integration over fibre orientation distributions. 2009.

45. Smith RE, Tournier J-D, Calamante F, Connelly ASIFT. Spherical-deconvolution informed filtering of tractograms. NeuroImage 2013;67:298–312.

46. Glasser MF, Coalson TS, Robinson EC, et al. A multi-modal parcellation of human cerebral cortex. Nature 2016;536:171–178.

47. Gleichgerrcht E, Fridriksson J, Rorden C, Bonilha L. Connectome-based lesion-symptom mapping (CLSM): a novel approach to map neurological function. NeuroImage 2017;16:461–467.

48. Xie T, He Y. Mapping the Alzheimer's brain with connectomics [Internet]. Front Psychiatry 2012;2:77.

49. Bioulac B, Burbaud P, Cazalets J-R, Gross C. Fonctions motrices. EMC - Neurolog 2004;1:277–329.

50. Rowe JB, Siebner HR. The motor system and its disorders. NeuroImage 2012;61:464–477.

51. Duda RO, Hart PE. Pattern classification and scene analysis [Internet]. A Wiley-Interscience Publication, New York: Wiley, 1973. Available from: http://adsabs.harvard.edu/abs/1973pcsa.book....D

52. Eccles JC. The cerebellum as a neuronal machine. Berlin: Springer Science & Business Media, 2013.

53. Buetefisch CM. Role of the contralesional hemisphere in post-stroke recovery of upper extremity motor function. Front Neurol 2015;6:214.

54. Silasi G, Murphy TH. Stroke and the connectome: how connectivity guides therapeutic intervention. Neuron 2014;83:1354–1368.

55. Jang SH, Seo YS, Lee SJ. Increased thalamocortical connectivity from the affected thalamus to the unaffected hemisphere in a stroke patient. Neural Regen Res 2020;15:1568.

56. Steiner L, Federspiel A, Slavova N, et al. Functional topography of the thalamo-cortical system during development and its relation to cognition. NeuroImage 2020;223:117361.

57. Yuan R, Di X, Taylor PA, et al. Functional topography of the thalamocortical system in human. Brain Struct Funct 2016;221:1971–1984.

58. Thompson DK, Loh WY, Connelly A, et al. Basal ganglia and thalamic tract connectivity in very preterm and full-term children; associations with 7-year neurodevelopment. Pediatr Res 2020;87:48–56.

59. Dinomais M, Minassian AT, Tuilier T, et al. Functional MRI comparison of passive and active movement: possible inhibitory role of supplementary motor area. NeuroReport 2009;20:1351–1355.

60. Mangia AL, Ursino M, Lannocca M, Cappello A. Transcallosal inhibition during motor imagery: analysis of a neural mass model. Front Comput Neurosci 2017;11:57.

61. Wardak C. The role of the supplementary motor area in inhibitory control in monkeys and humans. J Neurosci 2011;31:5181–5183.

62. Verfaellie M, Heilman KM. Response preparation and response inhibition after lesions of the medial frontal lobe. Arch Neurol 1987;44:1265–1271.

63. Holmefur M, Kits A, Bergström J, et al. Neuroradiology can predict the development of hand function in children with unilateral cerebral palsy. Neurorehabil Neural Repair 2013;27:72–78.

64. Ryll UC, Wagenaar N, Verhage CH, et al. Early prediction of unilateral cerebral palsy in infants with asymmetric perinatal brain injury - Model development and internal validation. Eur J Paediatr Neurol 2019;23:621–628.

65. Craig BT, Carlson HL, Kirton A. Thalamic diaschisis following perinatal stroke is associated with clinical disability. NeuroImage 2019;21:101660.

66. Scheck SM, Pannek K, Raffelt DA, et al. Structural connectivity of the anterior cingulate in children with unilateral cerebral palsy due to white matter lesions. NeuroImage 2015;9:498–505.

67. Staudt M. Reorganization after pre- and perinatal brain lesions*. J Anat 2010;217:469–474.

68. Kirton A. Modeling developmental plasticity after perinatal stroke: defining central therapeutic targets in cerebral palsy. Pediatr Neurol 2013;48:81–94.

69. Kong X-Z, Mathias SR, Guadalupe T, et al. Mapping cortical brain asymmetry in 17,141 healthy individuals worldwide via the ENIGMA Consortium. Proc Natl Acad Sci USA 2018;115:E5154–E5163.

70. Toga AW, Thompson PM. Mapping brain asymmetry. Nat Rev Neurosci 2003;4:37–48.

Supporting Information

Additional supporting information may be found online in the Supporting Information section at the end of the article.

Figure S1. The group lesion masks for the NAIS patients.
Table S1. The significant difference results of the structural connectivity metric comparison between controls and NAIS groups
Table S2. The significant difference results of the structural connectivity metric comparison between controls and NAIS groups.
Appendix S1.